An Improved Cuckoo Search Algorithm with Dynamic Parameters and Hybrid Distribution for Enhanced CLAHE

Sri Huning Anwariningsih
Department of Computer Science and Electronics, Gadjah Mada University, Yogyakarta, Indonesia | Department of Informatics, Sahid Surakarta University, Surakarta, Central Java, Indonesia
srihuninganwariningsih@mail.ugm.ac.id

Wahyono
Department of Computer Science and Electronics, Gadjah Mada University, Yogyakarta, Indonesia
wahyo@ugm.ac.id (corresponding author)

Raden Sumiharto
Department of Computer Science and Electronics, Gadjah Mada University, Yogyakarta, Indonesia
r_sumiharto@ugm.ac.id

Received: 20 February 2025 | Revised: 9 April 2025, 24 April 2025, and 3 May 2025 | Accepted: 8 May 2025

 DOI: https://doi.org/10.48084/etasr.10652

ABSTRACT

Contrast enhancement provides a more precise visualization of anatomical structures, improving diagnostic accuracy in medical images. One of the contrast enhancement methods, Contrast Limited Adaptive Histogram Equalization (CLAHE), often struggles with parameter optimization, leading to suboptimal image quality. Optimal parameter optimization is crucial to balancing contrast enhancement and detail preservation, necessitating robust optimization algorithms. The Cuckoo Search Algorithm (CSA) is well-suited for this task due to its strong global search capabilities and simplicity in handling complex optimization problems. CSA has two parameters, step size and discovery rate, which are often used as constants, resulting in sensitivity to problems, convergence rate, and an optimal solution that cannot be guaranteed simultaneously. To address these limitations, this study proposes an improved CSA, which, unlike conventional CSA with static parameters, introduces dynamic adjustments of the discovery rate (P_a) and step size (α), significantly improving exploration and exploitation capabilities. A hybrid distribution combining normal and uniform distributions is used for cuckoo selection and nest replacement, ensuring a balanced search process. The proposed method, called Dynamic Hybrid CSA (DH-CSA-CLAHE), was tested on MRI images of individuals with autism, showing superiority in MSE, PSNR, AMBE, SSIM, GMSD, and FSIM compared to CSA-CLAHE, PSO-CLAHE, and FA-CLAHE. The experimental results demonstrate the superior performance of the proposed method, achieving average PSNR, SSIM, and FSIM values of 45.54 dB, 0.97, and 0.9995, respectively, indicating excellent structural preservation and image quality. In addition, the method consistently produced the lowest MSE (3.73), AMBE (1.05), and GMSD (0.001) values, confirming its ability to effectively enhance contrast while minimizing distortion. These findings highlight the potential of DH-CSA-CLAHE as an effective tool for medical image preprocessing, contributing to improved diagnostic accuracy in clinical applications.

Keywords-Contrast Limited Adaptive Histogram Equalization (CLAHE); cuckoo search algorithm; dynamic discovery rate; dynamic step size; hybrid distribution

I. INTRODUCTION

Nowadays, MRI techniques have become one of the most crucial diagnostic examination methods in medical imaging. In [1], the most significant developments in the medical field in the last 25 years were identified, with the MRI and CT methods ranked at the top. MRI is widely used as a brain imaging technique because it does not expose the body to radiation, making it safe for the brain [2]. Although MRI techniques have several advantages, they also have limitations, as they produce images with low contrast. Since the analysis of low-contrast images is difficult for doctors and radiologists, image contrast enhancement is needed to facilitate human brain analysis [3]. By enhancing image contrast, physicians or radiologists can easily analyze detailed information [4-6].

One of the most widely used contrast enhancement techniques for improving the contrast of brain MRI images is Contrast Limited Adaptive Histogram Equalization (CLAHE) [3, 4, 7]. CLAHE can highlight parts of the image that need to be visible, effectively remove noise, and enhance local features, edges, and image contrast without losing relevant information [8]. Several studies have used CLAHE for medical image enhancement, such as brain images [9], breast [10], chest [11, 12], dental [13], liver [14], lung [14], retina [15], and others [16]. Meanwhile, the CLAHE method is applied to non-medical images, including rubber tree [4], sandstorm [3], satellite [17], and underwater [18] images. CLAHE has two crucial operating parameters: The Region Size (RS) and Clip Limit (CL). Improper hyperparameter selection can decrease image quality [19]. CLAHE often faces challenges in achieving optimal parameter settings. These limitations result in excessive contrast or loss of detail, reducing the overall quality of the enhanced images. However, optimizing CLAHE parameters is a complex task, as it requires a delicate balance between contrast improvement and preservation of fine image details.

Several research studies have explored optimization methods to address the challenge of determining the optimal parameters for CLAHE. Techniques such as Genetic Algorithms (GA), Particle Swarm Optimization (PSO) [20], and Firefly Algorithm (FA) [21] have shown promise in solving parameter optimization problems. GA, although robust, often requires significant computational resources due to its reliance on crossover and mutation processes that can result in slower convergence rates. Some studies utilized PSO to determine optimal CLAHE parameters and enhance image contrast quality [19, 20]. However, the number of tuning parameters in PSO is quite large. A primary issue with standard PSO is that the position and velocity vectors (particles) may become entrapped in locally optimal positions. Although faster in convergence, PSO tends to suffer from premature convergence, especially in high-dimensional or complex search spaces. The Firefly algorithm has also been used to determine the CLAHE parameters [22], but the results showed that the computation time was considerable and that contrast could not be maintained in the optic disc part of the retina. Similarly, the Firefly algorithm is based on attractiveness and distance metrics, but may struggle to balance exploration and exploitation effectively. The Firefly algorithm also has numerous tuning parameters that require adjustment, which can impact optimization performance.

Another optimization method that can be used is the Cuckoo Search Algorithm (CSA). CSA, inspired by the brood parasitism behavior of certain cuckoo species, has emerged as a competitive alternative due to its simplicity and strong global search capabilities. CSA has a main advantage over other optimization algorithms: the number of tuning parameters that need to be configured during initialization is fewer than that of others. CSA is also easy to implement, allowing inexperienced users to interact with it easily. Additionally, CSA has exploitation capabilities through random walks and explorations through Lévy Flight (LF). CSA can balance between local search strategies (exploitation) and the entire search space (exploration), can handle multicriteria optimization problems, and can converge faster [22, 23]. However, most CSA implementations use fixed parameters for two crucial parameters: discovery rate (P_a) and step size (α) at LF, which limit flexibility and reduce performance in highly dynamic search conditions.

Several studies have attempted to optimize CSA by adjusting its tuning parameters. In [24], the focus was on the improved cuckoo algorithm for adaptive adjustment of discovery probability. This method consisted of two states: the state discriminant parameter P_a, which is calculated by a Pareto optimal solution, and then the balance parameter P_{eb}, calculated by exploring and exploiting the equilibrium state. The performance of this method was analyzed using 10 benchmark functions. This study compared the proposed method only with CSA, specifically in terms of convergence speed, optimization ability, stability, and computational time. In [25], another attempt was introduced to improve CSA, focusing also solely on adaptive discovery probability, where the parameter used Double Mersenne Numbers (DMN). Additionally, this study focused exclusively on optimizing the CEC2017 benchmark function in the domain of mathematical optimization, without applying it to image processing.

Unlike previous studies, the proposed method introduces a new adaptive mechanism specifically designed for image contrast enhancement. The proposed method integrates the dynamic adjustment of the discovery rate (P_a) and step size (α) during optimization into the CSA. Additionally, a hybrid distribution mechanism combines normal and uniform distributions to enhance the selection of cuckoo candidates and nest replacement strategies. More importantly, the DH-CSA framework is tailored to the requirements of medical image enhancement, where striking a balance between contrast improvement and preservation of structural and color information is crucial. Furthermore, this study aimed to enhance the CSA to improve its ability to select optimal CLAHE parameters. By addressing the limitations of static parameters in CSA, this research aimed to achieve superior contrast enhancement and detail preservation in brain MRI images, particularly for applications in ASD analysis. The proposed method was evaluated using Image Quality Assessment (IQA) metrics. The proposed DH-CSA-CLAHE significantly improves adaptability, exploration and exploitation capabilities, and CLAHE parameter optimization. The main contributions of this study are:

1. Introduces a dynamic adjustment mechanism for the discovery rate (P_a) and step size (α), addressing the rigidity of static parameters in conventional CSA.
2. Develops a hybrid distribution that combines normal and uniform distributions to enhance cuckoo selection and nest replacement strategies, leading to improved search performance.
3. Integrates the enhanced DH-CSA-CLAHE framework into CLAHE parameter optimization, achieving significant improvements in contrast enhancement and detail preservation for brain MRI images.

II. CUCKOO SEARCH ALGORITHM

CSA was developed by Xin-She Yang and Suash Deb [26]. It is a modern metaheuristic algorithm inspired by the behavior of cuckoo bird parasites in laying their eggs, combined with LF behavior. The cuckoo bird does not incubate its eggs; instead, it places its eggs in the nests of other birds and removes the other eggs to increase the chances of its offspring hatching. If the original bird becomes aware of the presence of the foreign egg, there is the possibility of discarding the egg or making a new nest. LF is a random walk distributed by Lévy and is very helpful for CSA in the search because its search steps are increasingly wider. Using sufficient iterations, LF can find every point in the search domain, which means that it always finds the best solution [27]. CSA that uses LF has better accuracy than other optimization algorithms in determining the optimum point. CSA uses a balanced combination of local and global exploratory random walk, controlled by the switching parameter P_a. Recent studies have shown that CSA has the potential to be significantly more efficient and has a higher probability of finding the global optimum than PSO and GA [28]. CSA has two distinct advantages over algorithms such as GA: efficient random walks and balanced mixing. LFs are typically more efficient than other random-walk-based randomization techniques, making CSA significantly more effective in global search. CSA can guarantee global convergence.

CSA is based on the following three rules [19]: (i) each cuckoo lays one egg at a time and places its egg in a randomly chosen nest, (ii) the best nests with high-quality eggs are carried over to the next generation, and (iii) the number of available host nests is fixed, and the probability of an egg laid by a cuckoo being found by a host bird is denoted by $P_a \epsilon [0,1]$. In this case, the host bird can either discard the egg or leave the nest and build a new one elsewhere.

Like other nature-inspired algorithms, CS initiates its optimization process from the initialization step and proceeds to the iterative phase. CSA is an iterative process where the search aims to replace the cuckoo eggs (the solutions) in the nests with new and better eggs.

A. Initialization Phase

The search space and population size are first established at this step, assuming that the search space's dimensions are D and the population size is n. The nests are initialized with solutions (eggs). The i-th $\{i = 1, 2 \dots, N\}$ solution, X_i^0, is initialized as [19]:

$$X_i^0 = Lb + (Ub - Lb) \otimes rand(D) \quad (1)$$

where X_i^0 is i-th solution given by $X_i = [x_{i1}, x_{i2}, \dots, x_{iD}]$, Lb and Ub are the optimization problem's lower and upper bounds, respectively, and D is the dimension of the problem. The symbol $\otimes$ indicates entrywise multiplication. For each solution X_i, a fitness value is calculated for the given objective function $F(X_i)$ that measures the quality of solutions. The best fitness value among the initial population is denoted by F_{max}.

B. Iterative Phase

The iterative procedure ensures that nests with the best solutions survive from generation to generation involving the following steps. CSA combines global and local random walks.

1) Global Random

A global random walk is performed using an LF. At iteration $\{t = 1, 2, \dots\}$, the i-th solution x_i^{t+1} is generated from the previous solution x_i^t using the LF as follows, where the next solution is obtained using [29]:

$$x_i^{t+1} = x_i^t + \alpha \otimes Lévy(\lambda) \quad (2)$$

$$\alpha = \alpha_0 \otimes (X_j^t - X_i^t) \quad (3)$$

where, x_i^{t+1} is a new solution, $\alpha > 0$ is the stepsize (3) that depends on the dimension of the problem, and t represents the current generation number. $X_j^t (i \neq j)$ is a randomly selected solution. Most cases use $\alpha_0 = 0.01$ to enhance the search capability. $Lévy(\lambda)$ is a random walk derived from the Lévy distribution, as specified in (4), characterized by infinite variance and a mean [30]:

$$Lévy(s, \lambda) = \frac{\lambda \Gamma(\lambda) \sin(\frac{\pi\lambda}{2})}{\pi} * \frac{1}{s^{1+\lambda}}, \quad (s \gg s0>0) \quad (4)$$

In most problems, the Mantegna algorithm, a symmetric stable Lévy distribution, is used to generate the step length s as follows [22]:

$$s = \frac{U}{|V|^{1/\beta}} \quad (5)$$

where β is a parameter that is often considered $\beta = 1.5$ [31], λ $(1 \leq \lambda \leq 3)$, and the values of u and v are drawn from a Gaussian normal distribution, as in (6), with zero mean and variance σ^2.

$$u \sim N(0, \sigma_u^2), \quad v \sim N(0, \sigma_v^2) \quad (6)$$

where the values of σ_u and σ_v are given by:

$$\sigma_u = \left\{\frac{\Gamma(1+\beta) \sin(\pi\beta/2)}{\Gamma[(1+\beta)/2]\beta.2^{(\beta-1)/2}}\right\}^{1/\beta}, \ \sigma_v = 1 \quad (7)$$

where $\Gamma(x)$ is the gamma function defined as:

$$\Gamma(z) = \int_0^\infty x^{z-1} e^{-x} dx \quad (8)$$

A new solution's fitness is calculated using an objective function that measures the quality of solutions. If the fitness of the new solution is better than the old one, it replaces it.

2) Local Random Walk

A local random walk on CSA can be performed by considering the parameter P_a (abandon probability/discovery rate). The worst solutions are abandoned, and new solutions are generated as [30]:

$$x_i^{t+1} = x_i^t + \alpha.s \otimes H(P_a - \varepsilon) \otimes (x_j^t - x_k^t) \quad (9)$$

where x_j^t and x_k^t are two different solutions randomly selected with random permutations. $H(u)$ is the Heaviside function, ε is a random number using a uniform distribution, and s is the step size.

3) Finding the Best Fitness

The fitness of new solutions is calculated, and the best fitness, which corresponds to the best solution, is sorted and compared with F_{max}. If the current best fitness is better than F_{max}, the new best solution replaces the previous optimal solution. The iteration process is stopped if it meets the termination condition, namely, it reaches the specified maximum number of generations, and then the best solution is found. The pseudo-code of the original CSA is shown in [29].

The main shortcomings of the basic CSA are: (i) the need to calculate the host nest repeatedly because the initialization is based on a random strategy, (ii) the easy fall of the approach into the local optimal solution, (iii) the slow convergence rate, (iv) the use of fixed parameters for nest selection again leads to host generation imperfections, and (v) a boundary issue in host selection because of the LF random walk, which may cause the selection to go out of the boundary. To overcome these issues, this study proposes a dynamic and hybrid CSA to enhance the original one.

III. THE PROPOSED METHOD

The proposed DH-CSA-CLAHE method aims to improve the CSA using dynamic parameters and hybrid distribution selection. It is used to find the clip limit and region size parameters in the CLAHE method to improve contrast in MRI images. Figure 1 presents the overall process diagram of the proposed method.

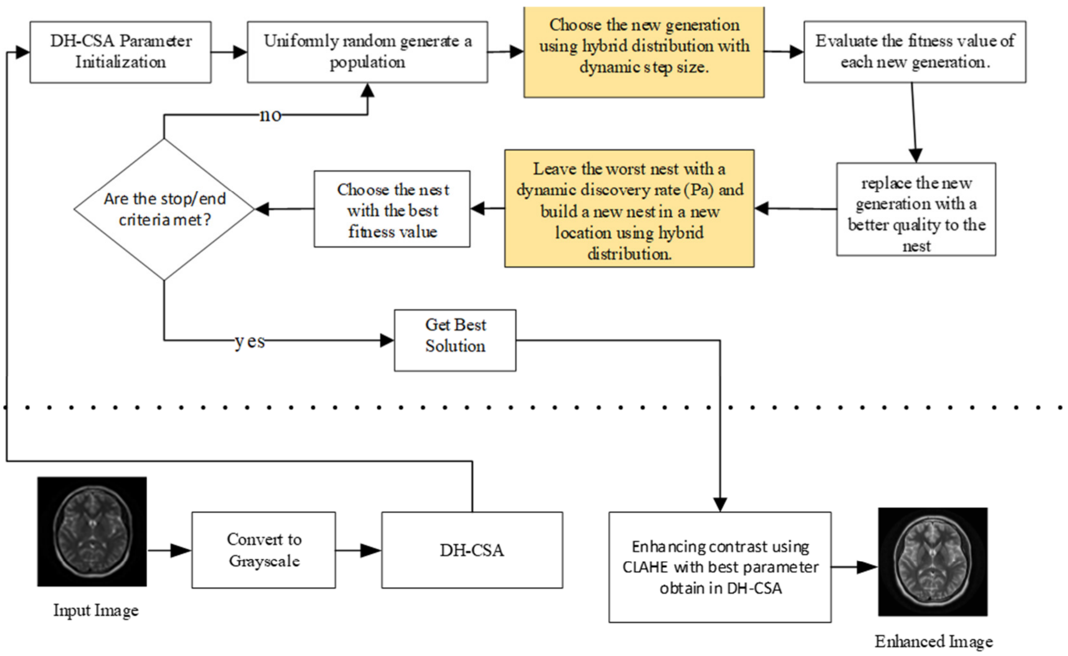

Fig. 1. Diagram of the proposed DH-CSA-CLAHE process.

A. Dynamic Discover Rate and Step Size

The step size and discovery rate parameters of the basic CSA are usually set to fixed values. Fixed values cause the number of host nests found to possibly repeat. The algorithm will struggle to converge if the fixed-step size value is too large. On the other hand, if the step size is too small, the algorithm will get stuck in a local solution. Changes in the value of P_a affect the performance of CSA [32]. The proposed method dynamically adjusts both parameters for each generation. Dynamic parameter tuning can increase the algorithm's convergence rate and result in an efficient search process for the best global position with minimal search operations [32].

The DH-CSA-CLAHE algorithm adopts a modified CSA method by adjusting the discovery rate and step size [33]. Dynamic parameters can enhance the algorithm's flexibility and optimize the exploration and exploitation of solutions [34]. In the DH-CSA-CLAHE method, the parameters of discovery rate and step size are modified as follows:

$$P_a = P \frac{CurrentIteration^k}{MaxIteration} a_{min} a_{max}{}_{a_{min}} \quad (10)$$

where $P_{a_{min}}$ and $P_{a_{max}}$ are the lower and upper limits of the discovery rate, and k controls the speed of change in P_a. If the value of k is greater than 1, then the changes are slower at the beginning of the iteration, thereby extending exploration. If the value of k is less than 1, the changes are faster, focusing on early exploitation. The more iterations that pass, P_a gradually decreases, allowing for broader exploration at the beginning and a focus on exploitation in the later iterations.

$$\alpha = a_{max} \exp(-\lambda(\frac{CurrentIteration}{MaxIteration}) \quad (11)$$

where α_{max} is the maximum initial step size and λ is the control coefficient for the rate of decrease of α. The exponential ensures that α decreases rapidly at the beginning and slowly approaches a small value as the iteration approaches the maximum. A larger step size at the start of the iteration allows for broader exploration, while a smaller step size in the later iterations facilitates exploitation.

Based on (10) and (11), the parameter modification aims to enhance the balance between exploration and exploitation. With this modification, the initial step uses a larger value for broad solution exploration, while the subsequent steps decrease to focus more on exploiting the best solutions. In (10), a linear decay approach is adopted to gradually reduce the value of P_a during the iteration process, and the use of $P_{a_{min}}$ and $P_{a_{max}}$ provides flexibility in setting the value range [35]. In the early iterations, P_a has a higher value approaching $P_{a_{max}}$. A high P_a allows more solutions to be randomly replaced, increasing the search space for exploration to find potential areas. In the iterations nearing the end, P_a decreases to $P_{a_{min}}$. A low P_a allows the algorithm to focus more on local exploitation to improve solutions around the global optimum. $P_{a_{min}}$ controls how much exploitation is performed at the end of the iterations. A low $P_{a_{min}}$ helps the algorithm narrow down the search space. Meanwhile, $P_{a_{max}}$ controls the initial exploration rate. A high $P_{a_{max}}$ value helps the algorithm explore the search space broadly.

B. Hybrid Distribution Selection

In addition to modifying the discovery rate and step size values, the proposed DH-CSA-CLAHE method also suggests applying a hybrid distribution at two critical stages in the optimization process: the selection of new solution generations and the replacement of solutions based on the discovery rate. In the original CSA, both processes are performed at random. Basic CSA employs a Gaussian normal distribution for global random walks and a uniform distribution for local random walks. The Gaussian distribution produces values concentrated around the mean, resulting in smaller step sizes, especially if the standard deviation σ is also small. This potentially causes the algorithm to fail to explore the search space broadly in the early iterations, which can lead to premature convergence. The Gaussian distribution often fails in global exploration because it cannot effectively produce significant steps compared to the Lévy distribution [29]. In addition, the uniform distribution has the characteristic of randomly generating new solutions within a fixed range, often lacking sufficient focus on the best solution. This results in less effective local exploitation, especially in the final iterations when the algorithm requires small, focused steps. The uniform distribution is less flexible for local exploitation than the normal distribution [36]. Research on the modification of this distribution has also led to improved CSA performance [37].

In the DH-CSA-CLAHE method, the adaptation of the standard deviation is performed dynamically using (12). This adaptation of the standard deviation is carried out to: (i) balance exploration and exploitation, (ii) enhance the stability and efficiency of convergence, and (iii) maximize the performance of the hybrid distribution.

$$std = std_{initial} * \left(1 - \frac{iteration}{MaxIteration}\right) \tag{12}$$

In the DH-CSA-CLAHE method, a hybrid distribution (a combination of normal and uniform distributions) is used to create new solutions (newCL and newRS). The hybrid distribution provides a 50% probability of choosing either the normal or uniform distribution to create a new solution, where the normal distribution uses the mean (μ) and standard deviation (σ) of the population, and the uniform distribution generates a new clip limit value randomly within the range $[0,1]$ and an integer region size value randomly within the range $[2,32]$. The range region size is determined based on previous research [38]. The determination of this range aims to expand the search area. The hybrid distribution algorithm for creating new solutions is presented in Algorithm 1. The hybrid distribution is also used to replace or discover new solutions (discovery process) in the population based on P_a.

```
Algorithm 1: Generate New Solution
Begin
If RandomValue()<0.5 Then
// Generate new solution using Normal
// Distribution
  newCL = NormDistr(meanCL,stdCL)
  newRS=
    ConvertToInt(NormDist(meanRS,stdRS))
Else
// Generate new solution using Uniform
// Distribution
  newCL = UniformDistribution(0.0, 1.0)
  newRS = UniformInteger(2, 32)
End If
// Ensure the new parameters are within
// valid ranges
newCL = Clamp(newCL, 0.0, 1.0)
newCL = Clamp(newRS, 2, 32)
Return (newCL, newRS)
End
```

C. Objective Function

The objective functions used are normalized entropy and SSIM. This selection is based on the consideration that entropy can express the richness of image information [39], while SSIM represents the similarity of luminance, contrast, and structure between the enhanced and the original images [40]. Normalized entropy helps measure the information diversity or uncertainty among images with varying pixel counts or intensity ranges and can be calculated using (13). Meanwhile, the second objective function, SSIM, is calculated using (14).

$$Ent_{norm} = \frac{\left(-\sum_{i=0}^{L-1} p(i)\log_2 p(i)\right)}{(\log_2 L)} \tag{13}$$

where L is the number of intensity levels, $p(i)$ is the probability of occurrence of pixel i intensity, and $log_2(L)$ denotes the base-2 logarithm of L, which represents the maximum achievable entropy when all pixel values have identical probabilities.

$$SSIM(x,y) = \frac{(2\mu_x\mu_y + C_1)(2\sigma_{xy} + C_2)}{({\mu_x}^2 + {\mu_y}^2 + C_1)({\sigma_x}^2 + {\sigma_y}^2 + C_2)} \tag{14}$$

where (x,y) denotes the input and enhanced images, respectively. Here, μ, σ, and C represent the mean intensity, the standard deviation, and the constant of the image.

The proposed method integrates objective functions into a singular scalar value using the weighted sum method [41]. Two distinct objective functions are employed to maximize both normalized entropy and SSIM, each allocated a weight of 0.5 (15). Based on experimental results, a weight of 0.5 for each element produced a competitive PSNR value, which was higher than the average PSNR of all the tested weight combinations.

$$F(x) = 0.5 * Ent_{norm} + 0.5 * SSIM \qquad (15)$$

The DH-CSA-CLAHE algorithm uses the converted input image as its input. It starts by setting the initial parameters of DH-CSA, which include the number of iterations, the population size, and the values of $P_{a_{min}}$, $P_{a_{max}}$, α_{max}, and λ. The next step is to generate the initial population, which is generated randomly within the specified boundaries, where the boundary of the clip limit is $[0.0, 1.0]$, and the boundary of the region size is $[2, 32]$. This process is repeated according to the population size. The next step involves selecting the new generation of cuckoos as the population's solution, using a hybrid distribution with a dynamic step size. The determination of the dynamic step size is based on (11). Each newly generated solution is evaluated using the objective function, in this study defined in (15). If the new solution is better than the old one, then it is updated. Some nests are selected to be replaced with new solutions based on P_a. New nests are created using a random search strategy by exchanging solutions among several selected nests. In this study, the discovery probability is dynamically adapted based on a hybrid distribution of normal and uniform distributions (10). All solutions are updated at this stage, and the best solution is stored. This process is repeated until the maximum number of iterations is reached. The algorithm stops if the stopping criteria are met (in this study, using the maximum number of iterations). The best solution found is considered optimal. In this case, the optimal solution is the best clip limit and region size values, which are then used as the best parameters in CLAHE to enhance the input image. The DH-CSA-CLAHE algorithm produces an output in the form of an enhanced image.

In this study, the initial parameters of the DH-CSA-CLAHE algorithm were chosen as follows: number of iterations $= 20$, population size =25, $P_{a_{min}}$= 0.1, $P_{a_{max}}$= 0.5, α_{max}=1, and λ= 0.05. These initial parameters were selected based on several considerations. Simulations showed that at $n = 25$ and $t = 20$, the CSA-CLAHE method had already converged. So in this study, the same values are also used. The selection of $P_{a_{min}}$ and $P_{a_{max}}$ refers to [29], which tested P_a values in the range of 0.0-0.5. This study also stated that in most cases, $\alpha = 1$ can be used [29]. The λ value is determined manually.

IV. RESULTS AND DISCUSSION

A. Dataset

The performance of DH-CSA-CLAHE was compared with the conventional CLAHE and WCSA methods [38]. This experiment used a public dataset from Autism Brain Imaging Data Exchange I (ABIDE I) MRI images [23], which contain MRI brain images of individuals diagnosed with Autism Spectrum Disorder (ASD). The analysis comprised 290 MRI brain images, encompassing both genders and various age categories, including children, adolescents, and adults. Furthermore, the DH-CSA-CLAHE method was also applied to low-contrast images from Kaggle to assess how well the proposed model performed. These images showed MRI scans of the abdomen, heart, and brain tumor.

B. Experimental Environment

The proposed method was implemented in Python with Visual Studio Code 1.91.0. The Python libraries used are NumPy for numerical operations and array manipulation, OpenCV for image processing, including the application of CLAHE, skimage for entropy measurement and image metrics, Pandas for data manipulation and analysis, time for measuring execution time, and math for basic and complex numerical operations. The following results are all obtained on a PC with an Intel Core i5-8250U CPU (1.80 GHz), 8 GB DDR4 RAM, and NVIDIA GeForce 930MX GPU.

C. Performance Analysis

The proposed method was also compared with CLAHE [28], CSA-CLAHE [38], PSO-CLAHE [20], and the Firefly Algorithm-CLAHE (FA-CLAHE) [21]. Figure 2 presents visual comparisons of some enhanced images from each method. In Figure 2, the improved image using CLAHE with CL = 2 and RS = 8×8 shows the resulting image, which has darker region details. The improved images using PSO-CLAHE mostly show visualizations with excessive contrast enhancement, although some images exhibit only moderate contrast improvement. This indicates a relatively high level of distortion from the PSO-CLAHE method. In contrast, the FA-CLAHE method effectively enhanced the contrast visually. However, some areas experienced a decrease in contrast, where some parts appeared darker, making the boundary between the black and white areas very clear. CSA-CLAHE also succeeded in enhancing contrast, but some areas remained dark. The DH-CSA-CLAHE method exhibited increased contrast and improved images with less distortion compared to the other optimization methods. DH-CSA-CLAHE also preserved local details more successfully.

Figure 3 presents a visual comparison of images resulting from low-contrast MRI, using the proposed and other methods. To make the comparison fairer, the number of PSO particles and FA fireflies was set equal to the number of CSA nests, which was 25. Meanwhile, the number of iterations was set to t =20. The three comparison methods also used the same objective function. The values of P_a and step size in CSA-CLAHE were set as constant values of 0.25 and 1.5. The dimensions for all methods were set to 3, with a clip limit range between 0 and 1 (inclusive) and a region size range between 2 and 32 (inclusive).

The performance of the proposed method was evaluated using several IQA evaluation metrics, specifically MSE, PSNR [19], AMBE [19], SSIM (14), FSIM [42], and GMSD [43] for 290 MRI images of ABIDE. PSNR measures image quality, with higher values indicating superior image quality. MSE assesses the sensitivity of errors in the enhanced image compared to the original image, with lower values indicating lower errors in the enhanced image compared to the original [15].

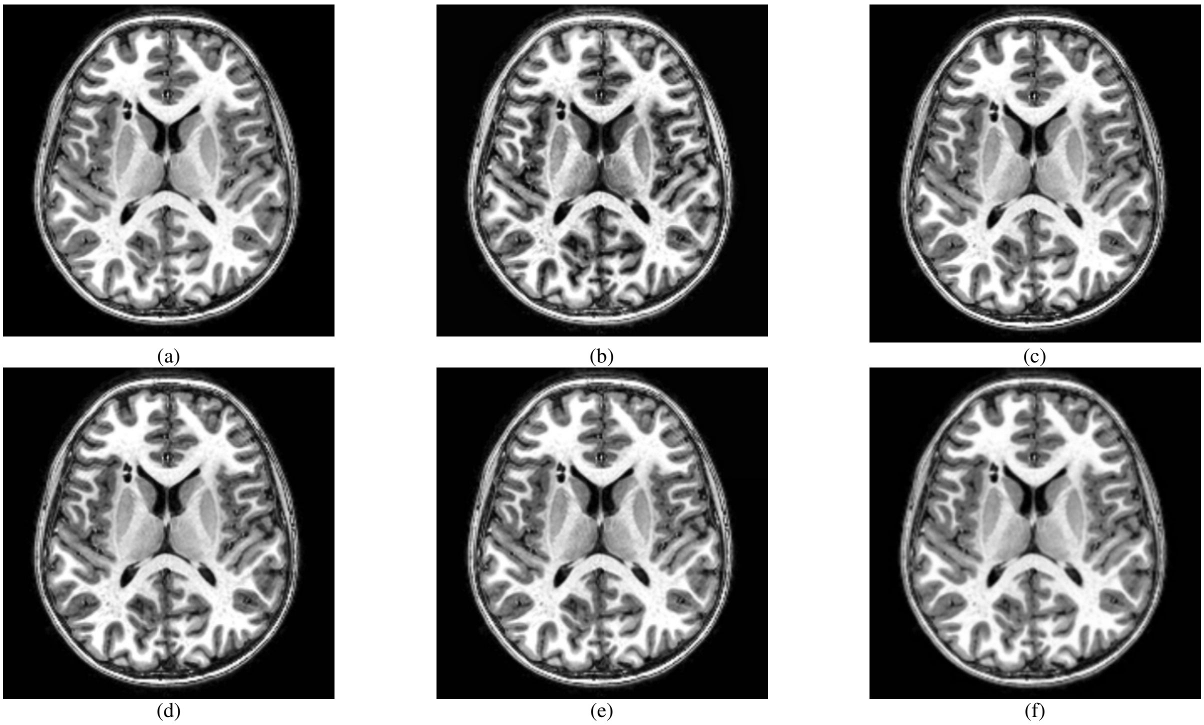

Fig. 2. Visual comparison of an ABIDE image: (a) Original Image, (b) conventional CLAHE (CL 2, RS=8×8), (c) PSO-CLAHE, (d) FA-CLAHE, (e) CSA-CLAHE, (f) DH-CSA-CLAHE.

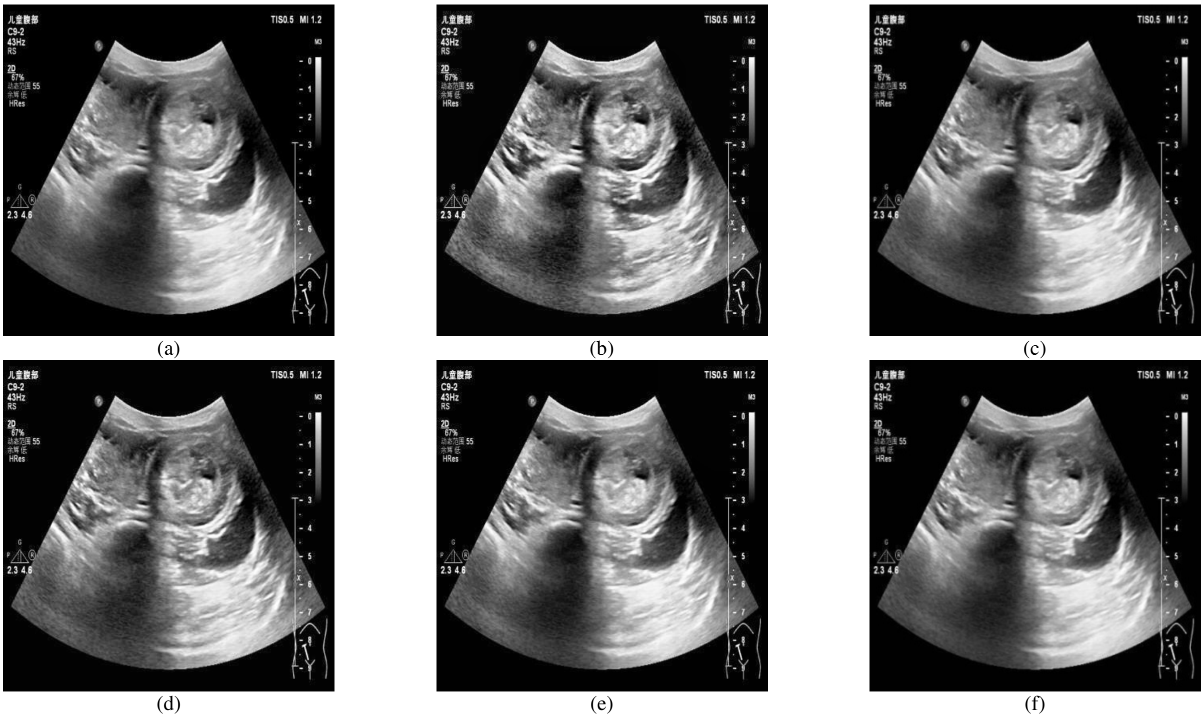

Fig. 3. Visual comparison of MRI image: (a) Original low contrast image, (b) Conventional CLAHE (CL 2, RS=8×8), (c) PSO-CLAHE, (d) FA-CLAHE, (e) CSA-CLAHE, (f) DH-CSA-CLAHE.

AMBE measures the absolute brightness disparity between the original and enhanced images, with lower values suggesting superior image brightness retention or better brightness preservation [19]. SSIM represents the luminance, contrast, and structure obtained from the enhanced image compared to the original. SSIM values range from 0 to 1, with a value of 1 or close to 1 indicating high structural similarity between the original and enhanced images. FSIM is used to measure the similarity between two images based on the important features captured by the Human Visual System (HVS). The FSIM index incorporates two factors: Phase Congruency (PC) and Gradient Magnitude (GM) derived from an image. FSIM is computed between the reference image and the distorted image and ranges from 0 to 1. The closer it gets to 1, the more the resulting image resembles the reference image [42]. GMSD is a metric that assesses the quality of an enhanced image by comparing its gradients (local intensity changes) with the original image. The enhancement process often alters the edges of the image. GMSD detects if the image is too smooth (losing edges) or too noisy (resulting in false edges). GMSD is very effective because it considers the gradient magnitude, which is closely related to human perception of edges, details, and structures in images. The GMSD values range from 0 to ∞. A GMSD of zero indicates perfect similarity with no distortion. The smaller the GMSD, the better the quality of the resulting image [43].

Table I compares the MSE, PSNR, AMBE, SSIM, GMSD, and FSIM values between the proposed and the other methods on ABIDE images. Table II presents the measurements on low-contrast MRI images, which comprise a total of 27 low-contrast MRI test images. For a deeper analysis, the performance comparison of the proposed method with others is also presented in graphs.

TABLE I. COMPARISON ON ABIDE IMAGES

Method	MSE	PSNR	AMBE	SSIM	GMSD	FSIM
CSA-CLAHE [38]	24.43	36.83	2.19	0.96	0.003	0.9969
PSO-CLAHE [20]	192.80	40.13	3.55	0.94	0.013	0.9908
FA-CLAHE [21]	65.69	30.57	3.47	0.91	0.014	0.9872
DH-CSA-CLAHE (proposed)	**3.73**	**45.54**	**1.05**	**0.97**	**0.001**	**0.9995**

TABLE II. COMPARISON ON LOW-CONTRAST MRI IMAGES

Method	Average Value		
	PSNR	AMBE	SSIM
CSA-CLAHE [38]	31.51	5.41	0.92
PSO-CLAHE [20]	37.34	3.51	0.93
FA-CLAHE [21]	27.71	7.32	0.81
DH-CSA-CLAHE (proposed)	**41.39**	**2.08**	**0.95**

As shown in Table I and Figure 4, based on the average PSNR values, the proposed method (DH-CSA-CLAHE) achieved the highest scores compared to all benchmark methods. Higher PSNR values indicate that the proposed method can produce superior image quality. Additionally, the proposed method yielded the lowest MSE values. In image enhancement, a low MSE value indicates that there is a minimal numerical error between the enhanced image and the original, meaning that the difference in pixel values between the enhanced image and the original is minimal. A low MSE indicates the preservation of the original or reference image's spatial structure information, including edges, textures, and patterns, following the enhancement process. This means that the enhanced image does not exhibit significant changes or distortions compared to the reference. The enhancement process only improves visual quality (for example, increasing contrast) without damaging the main content [44].

When examining the AMBE values, the proposed method yielded the best (smallest) AMBE value among all benchmark methods (Figure 5). This demonstrates that DH-CSA-CLAHE effectively preserves the image brightness while simultaneously minimizing noise. The proposed method also achieved the largest SSIM value, indicating a high structural similarity between the original and enhanced images. Figure 6 also reveals that DH-CSA-CLAHE achieved the highest FSIM value among all the compared methods. A higher FSIM suggests that the enhancement process effectively preserves important features of the original image, such as edges, textures, and patterns. This indicates that the proposed method effectively enhances visual quality without compromising important features and maintains spatial structure [42]. When examining the GMSD value, the proposed method achieved the best (lowest) score among all the compared methods (Figure 7). A low GMSD value indicates that the proposed method retains the enhanced image, preserving edges and structures that are similar to those in the original image. This suggests that the enhancement process is working effectively.

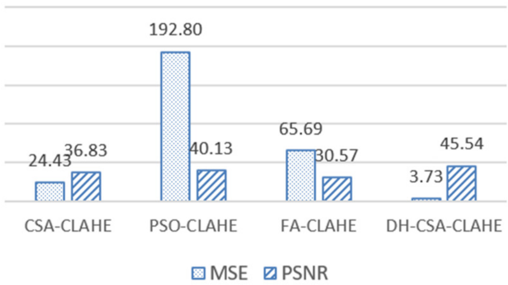

Fig. 4. Comparison of MSE and PSNR values.

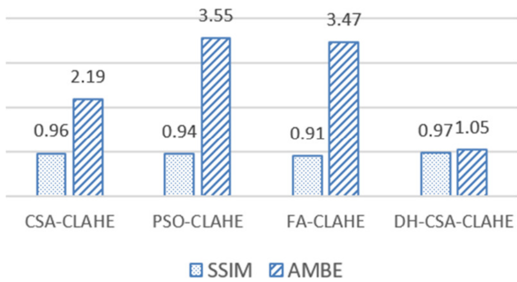

Fig. 5. Comparison of SSIM and AMBE values.

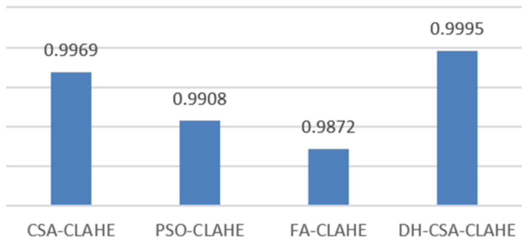

Fig. 6. Comparison of FSIM values.

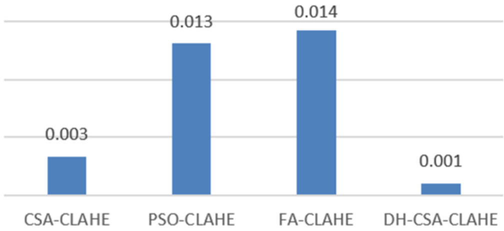

Fig. 7. Comparison of GMSD values.

All measurements confirm that the proposed method achieved superior performance compared to the other methods. The experimental results indicate that the proposed DH-CSA-CLAHE method achieved the lowest MSE, the highest PSNR, the highest SSIM, the lowest AMBE, the highest FSIM, and the lowest GMSD compared to the other methods. These results confirm that the proposed DH-CSA-CLAHE method effectively enhances image contrast while preserving the structural and color information of the original image. DH-CSA-CLAHE successfully enhances image contrast while effectively preserving both the structural and color information of the original images. The improvements in FSIM and GMSD further demonstrate the proposed method's capability to maintain fine details and texture information after enhancement. Furthermore, to ensure that the research results are reproducible and reliable, the test was conducted 5 times by calculating the mean, standard deviation (std), and confidence interval (CI) at a 95% confidence level for each evaluation metric.

TABLE III. STATISTICAL TESTING OF MODEL PERFORMANCE

Metrics	Mean	std	95% CI Lower	95% CI Upper
MSE	3.73	4.97E-16	3.732359	3.732359
PSNR	45.54	0	-	-
SSIM	0.97	0	-	-
AMBE	1.05	0	-	-
GMSD	0.00	0	-	-
FSIM	0.9995	1.24E-16	0.999538	0.999538

Based on the results obtained (Table III), the variation in the results for each metric is shown to be minimal, indicated by the standard deviation values approaching zero. The small CIs for each metric also suggest that the experimental results are consistent and stable across all trials. The FSIM value, with a 95% CI of 0.9995, indicates that the results exhibit excellent visual quality, consistent across all tests. The SSIM, PSNR, and GMSD values all show the same thing: stable and almost perfect results. This demonstrates the reliability and repeatability of the proposed method.

The Computational Time (CT) was also compared to ensure a fairer comparison (Figure 8), as time is a critical factor in computer applications and optimization methods. The CSA-CLAHE and PSO-CLAHE methods exhibited the fastest processing times, at 10.30 s and 10.43 s, respectively. FA-CLAHE required a longer time of 74.46 s due to the additional complexity introduced by the Firefly optimization process. However, the DH-CSA-CLAHE method showed a substantially longer computation time of 1517.03 s. This drastic increase is primarily caused by the nested hybrid optimization strategy used in DH-CSA-CLAHE that iteratively combines CSA and other mechanisms during the clip-limit and region size selection processes. Since the hybrid search procedure is more complex, it requires more iterations and consumes more computing power than single or more straightforward metaheuristic methods. Although the DH-CSA-CLAHE method demonstrates superior performance in terms of image quality metrics (MSE, PSNR, SSIM, FSIM, AMBE, and GMSD), the trade-off is a significantly higher computational cost. This limitation suggests that DH-CSA-CLAHE is more suitable for offline applications or scenarios where CT is not a critical constraint. Real-time or time-sensitive applications may prefer lighter methods, such as CSA-CLAHE or PSO-CLAHE, despite their lower enhancement performance.

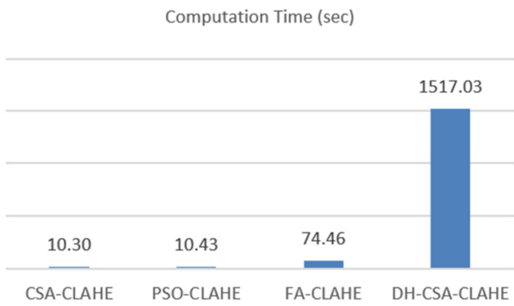

Fig. 8. Comparison of Computational Time (CT).

V. CONCLUSION

This research introduced DH-CSA-CLAHE, a novel extension of CSA specifically designed for adaptive contrast enhancement in MRI images. The proposed method introduces two significant innovations: (i) the dynamic adjustment of both discovery probability and step size, and (ii) the incorporation of a hybrid distribution strategy to generate new solutions more effectively. The objective functions used, normalized entropy and SSIM, are integrated using a weighted sum function to guide optimization. The proposed method determines the clip limit and the region size parameters of CLAHE to adaptively enhance the contrast of MRI images. Experimental results on the ABIDE dataset showed that DH-CSA-CLAHE achieved superior performance compared to other methods (CLAHE, CSA-CLAHE, PSO-CLAHE, and FA-CLAHE) as demonstrated by lower MSE, AMBE, and GMSD values, and higher PSNR, SSIM, and FSIM values. Furthermore, visual assessment confirmed that the proposed method can effectively preserve structural details and suppress over-enhancement and distortion, which are crucial for reliable medical image interpretation. Compared to other optimization-based CLAHE approaches, the dual adaptation of dynamic parameters and hybrid distribution in DH-CSA-CLAHE offers a more robust and flexible solution for contrast enhancement tasks. Nevertheless, the method still suffers from a relatively long computational time due to its multistage optimization process. Future studies will focus on reducing computational time and extending the validation of DH-CSA-CLAHE to other medical imaging modalities and general image enhancement tasks.

ACKNOWLEDGMENT

The authors would like to thank the Ministry of Research and Higher Education of the Republic of Indonesia through Gadjah Mada University, which has funded this research with contract numbers 1907/UN1/DITLIT/Dit-Lit/PT.01.03/2022.

REFERENCES

[1] H. I. Ashiba *et al.*, "Enhancement of IR images using histogram processing and the Undecimated additive wavelet transform," *Multimedia Tools and Applications*, vol. 78, no. 9, pp. 11277–11290, May 2019, https://doi.org/10.1007/s11042-018-6545-9.

[2] Z. Ullah, S. H. Lee, and D. An, "Histogram Equalization based Enhancement and MR Brain Image Skull Stripping using Mathematical Morphology," *International Journal of Advanced Computer Science and Applications*, vol. 11, no. 3, 2020, https://doi.org/10.14569/IJACSA.2020.0110372.

[3] K. Mayathevar, M. Veluchamy, and B. Subramani, "Fuzzy color histogram equalization with weighted distribution for image enhancement," *Optik*, vol. 216, Aug. 2020, Art. no. 164927, https://doi.org/10.1016/j.ijleo.2020.164927.

[4] B. Subramani and M. Veluchamy, "Fuzzy Gray Level Difference Histogram Equalization for Medical Image Enhancement," *Journal of Medical Systems*, vol. 44, no. 6, Jun. 2020, Art. no. 103, https://doi.org/10.1007/s10916-020-01568-9.

[5] D. Susilo and Wahyono, "An Analysis of Image Enhancement Effects on Convolutional Neural Network-based Pulmonary Tuberculosis Detection," *E3S Web of Conferences*, vol. 465, 2023, Art. no. 02054, https://doi.org/10.1051/e3sconf/202346502054.

[6] Wahyono, "Analisis Pengaruh Image Enhancement Pada Pendeteksian COVID-19 Berbasis Citra X-Ray," *Techno.Com*, vol. 22, no. 1, pp. 186–194, Feb. 2023, https://doi.org/10.33633/tc.v22i1.7195.

[7] M. J. Alwazzan, M. A. Ismael, and A. N. Ahmed, "A Hybrid Algorithm to Enhance Colour Retinal Fundus Images Using a Wiener Filter and CLAHE," *Journal of Digital Imaging*, vol. 34, no. 3, pp. 750–759, Jun. 2021, https://doi.org/10.1007/s10278-021-00447-0.

[8] M. Ge, Q. Hong, and L. Zhang, "A Hybrid DCT-CLAHE Approach for Brightness Enhancement of Uneven-illumination Underwater Images," in *Proceedings of the 2018 2nd International Conference on Video and Image Processing*, Hong Kong, Dec. 2018, pp. 123–127, https://doi.org/10.1145/3301506.3301539.

[9] G. Gao, H. Lai, Y. Liu, L. Wang, and Z. Jia, "Sandstorm image enhancement based on YUV space," *Optik*, vol. 226, Jan. 2021, Art. no. 165659, https://doi.org/10.1016/j.ijleo.2020.165659.

[10] R. P. R. Chegireddy and A. Srinagesh, "A Novel Method for Human MRI Based Pancreatic Cancer Prediction Using Integration of Harris Hawks Varients & VGG16: A Deep Learning Approach," *Informatica*, vol. 47, no. 1, May 2023, https://doi.org/10.31449/inf.v47i1.4433.

[11] P. Singh, R. Mukundan, and R. De Ryke, "Feature Enhancement in Medical Ultrasound Videos Using Contrast-Limited Adaptive Histogram Equalization," *Journal of Digital Imaging*, vol. 33, no. 1, pp. 273–285, Feb. 2020, https://doi.org/10.1007/s10278-019-00211-5.

[12] B. S. Min, D. K. Lim, S. J. Kim, and J. H. Lee, "A Novel Method of Determining Parameters of CLAHE Based on Image Entropy," *International Journal of Software Engineering and Its Applications*, vol. 7, no. 5, pp. 113–120, Sep. 2013, https://doi.org/10.14257/ijseia.2013.7.5.11.

[13] B. Joda and Z. Dereboylu, "Digital mammogram enhancement based on automatic histogram clipping," in *2017 9th International Conference on Computational Intelligence and Communication Networks (CICN)*, Sep. 2017, pp. 34–38, https://doi.org/10.1109/CICN.2017.8319351.

[14] S. S. M. Sheet, T. S. Tan, M. A. As'ari, W. H. W. Hitam, and J. S. Y. Sia, "Retinal disease identification using upgraded CLAHE filter and transfer convolution neural network," *ICT Express*, vol. 8, no. 1, pp. 142–150, Mar. 2022, https://doi.org/10.1016/j.icte.2021.05.002.

[15] B. Sree Vidya and E. Chandra, "Triangular Fuzzy Membership-Contrast Limited Adaptive Histogram Equalization (TFM-CLAHE) for Enhancement of Multimodal Biometric Images," *Wireless Personal Communications*, vol. 106, no. 2, pp. 651–680, May 2019, https://doi.org/10.1007/s11277-019-06184-6.

[16] B. Subramani and M. Veluchamy, "Fuzzy contextual inference system for medical image enhancement," *Measurement*, vol. 148, Dec. 2019, Art. no. 106967, https://doi.org/10.1016/j.measurement.2019.106967.

[17] S. Mohan and T. R. Mahesh, "Particle Swarm Optimization based Contrast Limited enhancement for mammogram images," in *2013 7th International Conference on Intelligent Systems and Control (ISCO)*, Coimbatore, Tamil Nadu, India, Jan. 2013, pp. 384–388, https://doi.org/10.1109/ISCO.2013.6481185.

[18] S. Anilkumar, P. R. Dhanya, A. A. Balakrishnan, and M. H. Supriya, "Algorithm for Underwater Cable Tracking Using CLAHE based Enhancement," in *2019 International Symposium on Ocean Technology (SYMPOL)*, Ernakulam, India, Dec. 2019, pp. 129–137, https://doi.org/10.1109/SYMPOL48207.2019.9005273.

[19] U. Kuran and E. C. Kuran, "Parameter selection for CLAHE using multi-objective cuckoo search algorithm for image contrast enhancement," *Intelligent Systems with Applications*, vol. 12, Nov. 2021, Art. no. 200051, https://doi.org/10.1016/j.iswa.2021.200051.

[20] M. Núñez *et al.*, "Particle swarm optimization applied to parameter tuning of clahe based on entropy and structural similarity index," *Journal of Computational Interdisciplinary Sciences*, vol. 5, 2014.

[21] K. G. Dhal and S. Das, "Colour retinal images enhancement using modified histogram equalisation methods and firefly algorithm," *International Journal of Biomedical Engineering and Technology*, vol. 28, no. 2, 2018, Art. no. 160, https://doi.org/10.1504/IJBET.2018.094725.

[22] P. P. Prajapati and M. V. Shah, "Performance Estimation of Differential Evolution, Particle Swarm Optimization and Cuckoo Search Algorithms," *International Journal of Intelligent Systems and Applications*, vol. 10, no. 6, pp. 59–67, Jun. 2018, https://doi.org/10.5815/ijisa.2018.06.07.

[23] "ABIDE - Autism Brain Imaging Data Exchange." http://fcon_1000.projects.nitrc.org/indi/abide/.

[24] W. Kun, J. Han, K. M. Abid Ali, and L. Xiaofeng, "Improved Cuckoo Algorithm for Adaptive Adjustment of Discovery Probability," in *2019 Chinese Control And Decision Conference (CCDC)*, Nanchang, China, Jun. 2019, pp. 5873–5878, https://doi.org/10.1109/CCDC.2019.8833285.

[25] M. Reda, M. Elhosseini, A. Haikal, and M. Badawy, "A novel cuckoo search algorithm with adaptive discovery probability based on double Mersenne numbers," *Neural Computing and Applications*, vol. 33, no. 23, pp. 16377–16402, Dec. 2021, https://doi.org/10.1007/s00521-021-06236-8.

[26] R. C. Gonzalez, *Digital Image Processing*, 4th ed. Pearson Education, 2019.

[27] S. M. Pizer, J. B. Zimmerman, and E. V. Staab, "Adaptive grey level assignment in CT scan display," *Journal of computer assisted tomography*, vol. 8, no. 2, pp. 300–305, Apr. 1984.

[28] K. Zuiderveld, "Contrast Limited Adaptive Histogram Equalization," in *Graphics Gems*, Elsevier, 1994, pp. 474–485.

[29] X. S. Yang and S. Deb, "Cuckoo Search via Lévy flights," in *2009 World Congress on Nature & Biologically Inspired Computing (NaBIC)*, Coimbatore, India, 2009, pp. 210–214, https://doi.org/10.1109/NABIC.2009.5393690.

[30] X. S. Yang, Nature-Inspired Optimization Algorithms. Academic Press, 2020.

[31] A. Kaveh and T. Bakhshpoori, "Optimum design of steel frames using Cuckoo Search algorithm with Lévy flights," *The Structural Design of Tall and Special Buildings*, vol. 22, no. 13, pp. 1023–1036, 2013, https://doi.org/10.1002/tal.754.

[32] S. Walton, O. Hassan, K. Morgan, and M. R. Brown, "Modified cuckoo search: A new gradient free optimisation algorithm," *Chaos, Solitons & Fractals*, vol. 44, no. 9, pp. 710–718, Sep. 2011, https://doi.org/10.1016/j.chaos.2011.06.004.

[33] M. Shehab, A. T. Khader, and M. A. Al-Betar, "A survey on applications and variants of the cuckoo search algorithm," *Applied Soft Computing*,

vol. 61, pp. 1041–1059, Dec. 2017, https://doi.org/10.1016/j.asoc.2017.02.034.

[34] B. Sahu, P. K. Das, and R. Kumar, "A modified cuckoo search algorithm implemented with SCA and PSO for multi-robot cooperation and path planning," *Cognitive Systems Research*, vol. 79, pp. 24–42, Jun. 2023, https://doi.org/10.1016/j.cogsys.2023.01.005.

[35] S. D. Prestwich, S. A. Tarim, and R. Rossi, "Intermittency and obsolescence: A Croston method with linear decay," *International Journal of Forecasting*, vol. 37, no. 2, pp. 708–715, Apr. 2021, https://doi.org/10.1016/j.ijforecast.2020.08.010.

[36] I. Fister, D. Fister, and I. Fister, "A comprehensive review of cuckoo search: variants and hybrids," *International Journal of Mathematical Modelling and Numerical Optimisation*, vol. 4, no. 4, 2013, Art. no. 387, https://doi.org/10.1504/IJMMNO.2013.059205.

[37] Y. Yuan, L. Wang, Q. Zhou, W. Xiao, L. Wang, and Y. Zhong, "Cuckoo Search Algorithm with Normal Distribution and Its Application in Lychee Image Segmentation," in *2023 9th International Conference on Systems and Informatics (ICSAI)*, Changsha, China, Dec. 2023, pp. 1–7, https://doi.org/10.1109/ICSAI61474.2023.10423367.

[38] S. H. Anwariningsih, Wahyono, and R. Sumiharto, "Enhancing Contrast Limited Adaptive Histogram Equalization Using Weighted Sum Cuckoo Search Algorithm," *ICIC Express Letters*, vol. 19, no. 5, pp. 475–483, 2025, https://doi.org/10.24507/icicel.19.05.475.

[39] H. T. R. Kurmasha, A. F. H. Alharan, C. S. Der, and N. H. Azami, "Enhancement of Edge-based Image Quality Measures Using Entropy for Histogram Equalization-based Contrast Enhancement Techniques," *Engineering, Technology & Applied Science Research*, vol. 7, no. 6, pp. 2277–2281, Dec. 2017, https://doi.org/10.48084/etasr.1625.

[40] R. Y. Lad, S. Mapari, and F. N. Sibai, "A Novel Approach to Image Classification for Detecting Abnormalities in Neuroimages based on the Structural Similarity Index Measure," *Engineering, Technology & Applied Science Research*, vol. 14, no. 5, pp. 17382–17387, Oct. 2024, https://doi.org/10.48084/etasr.8384.

[41] R. T. Marler and J. S. Arora, "The weighted sum method for multi-objective optimization: new insights," *Structural and Multidisciplinary Optimization*, vol. 41, no. 6, pp. 853–862, Jun. 2010, https://doi.org/10.1007/s00158-009-0460-7.

[42] L. Zhang, L. Zhang, X. Mou, and D. Zhang, "FSIM: A Feature Similarity Index for Image Quality Assessment," *IEEE Transactions on Image Processing*, vol. 20, no. 8, pp. 2378–2386, Aug. 2011, https://doi.org/10.1109/TIP.2011.2109730.

[43] W. Xue, L. Zhang, X. Mou, and A. C. Bovik, "Gradient Magnitude Similarity Deviation: A Highly Efficient Perceptual Image Quality Index," *IEEE Transactions on Image Processing*, vol. 23, no. 2, pp. 684–695, Feb. 2014, https://doi.org/10.1109/TIP.2013.2293423.

[44] D. Asamoah, E. Ofori, S. Opoku, and J. Danso, "Measuring the Performance of Image Contrast Enhancement Technique," *International Journal of Computer Applications*, vol. 181, no. 22, pp. 6–13, Oct. 2018, https://doi.org/10.5120/ijca2018917899.